Microstrip Realization of Generalized Chebyshev Filters With Box-Like Coupling Schemes

Ching-Ku Liao, Pei-Ling Chi, and Chi-Yang Chang, *Member, IEEE*

***Abstract*—This paper presents generalized Chebyshev microstrip filters with box-like coupling schemes. The box-like coupling schemes taken in this paper include a doublet, extended doublet, and fourth-order box section. The box-like portion of the coupling schemes is implemented by an E-shaped resonator. Synthesis and realization procedures are described in detail. The example filters show an excellent match to the theoretical responses.**

***Index Terms*—Bandpass filters, design, elliptic filters, resonator filters, transmission zero.**

I. Introduction

THE microstrip filters with a generalized Chebyshev response attract considerable attention due to its light weight, easy fabrication, and ability to generate finite transmission zeros for sharp skirts. In the literature, most of them are based on cross-coupled schemes such as a cascade trisection and cascade quadruplet. Some representative examples of cross-coupled microstrip filters are available in [1].

Recently, with the progress of the synthesis technique, new coupling schemes such as the "doublet," "extended doublet," and "box section" are introduced [2]–[4]. As shown in Fig. 1, these coupling schemes have a box-like center portion so we refer to them in this paper as box-like coupling schemes. These coupling schemes impact the filter design since they not only provide new design possibilities, but also exhibit some unique and attractive properties. They differ from the conventional cascade trisection and cascade quadruplet mainly on two aspects. First, there are two main paths for the signal from source to load, while there is only one main path in the case of cascade trisection and cascade quadruplet. Second, the configuration of the doublet and box section exhibit the zero-shifting property, which makes it possible to shift the transmission zero from one side of the passband to the other side simply by changing the resonant frequencies of the resonator while keeping other coupling coefficients unchanged. The zero-shifting property implies that the similar physical layout can implement a filter with a transmission zero at the lower stopband or at the upper stopband,

Manuscript received July 21, 2006; revised October 4, 2006. This work was supported in part by the National Science Council, R.O.C., under Grant NSC 95-2752-E-009-003-PAE and Grant NSC 95-2221-E-009-042-MY3.

C.-K. Liao and C.-Y. Chang are with the Department of Communication Engineering, National Chiao Tung University, Hsinchu 300, Taiwan, R.O.C. (e-mail: ching.cm92g@nctu.edu.tw; mhchang@cc.nctu.edu.tw).

P.-L. Chi is with the Department of Electrical Engineering, University of California at Los Angeles, Los Angeles, CA 90024 USA.

Color versions of one or more of the figures in this paper are available online at http://ieeexplore.ieee.org.

Digital Object Identifier 10.1109/TMTT.2006.888580

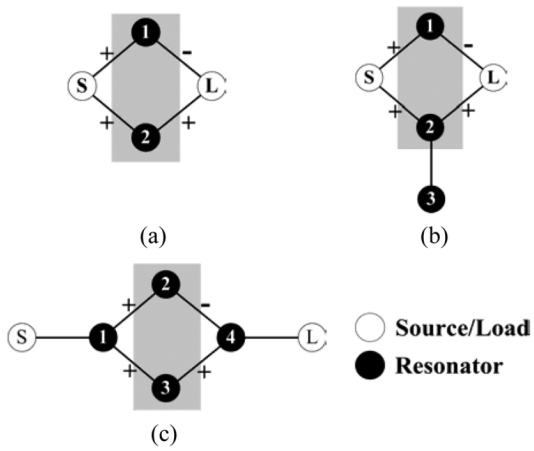

Fig. 1. Basic box-like coupling schemes for generalized Chebyshev-response filters discussed in this paper. (a) Doublet. (b) Extended doublet. (c) Box section. (The gray area is realized by the proposed E-shaped resonator.)

which is not feasible on the conventional trisection configuration. Besides, the third-order extended-doublet configuration, as shown in Fig. 1(b), exhibits one pair of finite transmission zeros as that of a cross-coupled quadruplet filter [5]. Pairs of finite transmission zeros can be used to improve the selectivity of the filter or flatten the in-band group delay. However, to the authors' knowledge, only a few studies in the literature are focused on realization of the coupling schemes shown in Fig. 1 with a microstrip line [6], [7].

An important property of the schemes in Fig. 1 is that one of the coupling coefficients on the two main paths must be negative while others are positive. The simplest way to obtain the required negative sign is to use higher order resonance [3], [7]. Unfortunately, higher order resonance leads to a spurious resonance in the lower stopband. Instead of using higher order resonance, loop resonators are arranged carefully to satisfy the required sign of coupling coefficients for the box-section configuration [5]. However, a similar method cannot apply to the doublet or extended doublet. To overcome these difficulties, an E-shaped resonator, as shown in Fig. 2(a), is proposed in this paper to implement the required coupling signs.

The E-shaped resonator can achieve the required magnitude and sign of the coupling schemes shown in Fig. 1. As shown in Fig. 2(a), the E-shaped resonator comprises a hairpin resonator and an open stub on its center plane. This symmetric structure can support two modes, i.e., an even mode and odd mode. Thus, the source and load are coupled to both modes of the E-shaped resonator. That is, even though only one physical path exists between source and load, there are two electrical paths between them. Consequently, the layout in Fig. 2(a) can be

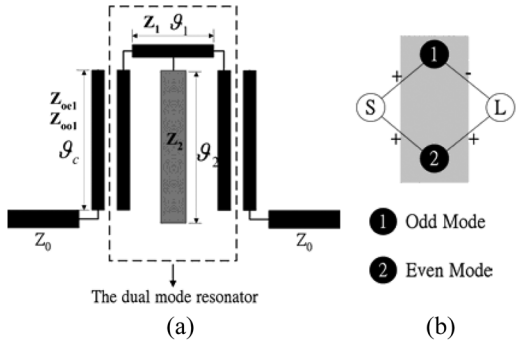

Fig. 2. Doublet filter. (a) Proposed layout (gray area indicate the E-shaped resonator). (b) Corresponding coupling scheme.

modeled by the coupling scheme, a doublet, shown in Fig. 2(b). The doublet filter illustrates how a E-shaped resonator directly couples to external feeding network. Furthermore, based on the proposed E-shaped resonator, filters with an extended-doublet and a box-section configuration can be realized as well. The E-shaped resonator can use either its even mode or odd mode to couple an extra resonator. Thus, the extended-doublet configuration in Fig. 1(b) is achievable. Besides, the E-shaped resonator can couple to external resonators with two of its modes simultaneously and forms the box-section configuration in Fig. 1(c). The feasibility of realization of the basic coupling schemes in Fig. 1 with the proposed E-shaped resonator makes it possible to realize a class of coupled microstrip filters in a unified approach.

II. Circuit Modeling

A. Filters in the Doublet Configuration

The E-shaped resonator filter in Fig. 2(a) was originally reported in [8]. In [8], the E-shaped resonator was not modeled as a two-mode resonator. Instead, the circuit was modeled as two quarter-wavelength resonators with a tapped open stub in the center plane. The open stub is considered as a K-inverter between two quarter-wavelength resonators to control the coupling strength, and as a quarter-wave open stub to generate a transmission zero at the desired frequency. However, the filter cannot be designed with a prescribed quasi-elliptic response since there is no suitable prototype corresponding to the circuit model in [8].

In this paper, a doublet, as shown in Fig. 2(b), is used to model the circuit in Fig. 2(a). In Fig. 2(b), resonator 1 represents the odd-mode resonance, where the center plane of the E-shaped resonator is an electric wall (E-plane). On the other hand, resonator 2 represents even-mode resonance, where the center plane of the E-shaped resonator is a magnetic wall (H-plane). With the notation shown in Fig. 2(b), the corresponding coupling matrix M can be written down as [3]

$$M = \begin{bmatrix} 0 & M_{S1} & M_{S2} & 0 \\ M_{S1} & M_{11} & 0 & M_{1L} \\ M_{S2} & 0 & M_{22} & M_{2L} \\ 0 & M_{1L} & M_{2L} & 0 \end{bmatrix}. \tag{1}$$

There are some interesting properties of the doublet filter in Fig. 2(a). First, since the E-shaped resonator exhibits symmetry, the relationship $M_{S1} = -M_{1L}$ and $M_{S2} = M_{2L}$ holds. Second, $|M_{S1}| > |M_{S2}|$ is always true for this structure since the coupling strength between the odd mode and external feeding network is always larger than that of the even mode.

To get more insight of how to control a transmission zero of a doublet filter in this configuration, an explicit expression relating the coupling elements and the transmission zero Ω is provided in a low-pass prototype as follows:

$$\Omega = \frac{\left(M_{11}M_{S2}^2 - M_{22}M_{S1}^2\right)}{\left(M_{S1}^2 - M_{S2}^2\right)}. \tag{2}$$

Note that the mapping between normalized frequency ω' and actual frequency f is $\omega' = (f/f_0 - f_0 - f_0/f)\Delta f/f_0$, where f_0 and Δf are center frequency and bandwidth of a filter, respectively.

Based on the (2), observations are summarized as follows.

1) The transmission zero is always located at finite frequency since $M_{S1} \neq M_{S2}$. In other words, the structure exhibits finite transmission zero inherently.
2) The transmission zero can be moved from the upper stopband to lower stopband, or vice versa, by changing the sign of M_{11} and M_{22} simultaneously. This property makes it possible to generate upper stopband or lower stopband finite transmission zero with similar structure.
3) If $M_{11} > 0$ and $M_{22} < 0$, Ω would be greater than zero. In a more explicit expression, M_{11} and M_{22} can be related to the resonant frequencies of odd mode f_{odd} and even mode f_{even}, respectively by the following equations:

$$f_{\text{odd}} = f_0\left(1 - \frac{M_{11} \times \Delta f}{2f_0}\right) \tag{3}$$

$$f_{\text{even}} = f_0\left(1 - \frac{M_{22} \times \Delta f}{2f_0}\right) \tag{4}$$

   where f_0 and Δf are the center frequency and bandwidth of a filter, respectively; i.e., if $f_{\text{odd}} < f_0$ and $f_{\text{even}} > f_0$, the transmission zero would be on the upper stopband.
4) If $M_{11} < 0$ and $M_{22} > 0$, Ω would be smaller than zero; i.e., if $f_{\text{odd}} > f_0$ and $f_{\text{even}} > f_0$, the transmission zero would be on the lower stopband.

To get the related electrical parameters indicated in Fig. 2(a), one can take the following procedures. First, synthesize a coupling matrix M corresponding to the prescribed response by methods provided in [7]. Then consider parameters concerning the odd mode only by removing the open stub on the center plane. Once the open stub is removed, the circuit becomes a first-order hairpin filter. The first-order hairpin filter can be synthesized by the conventional method [8] with the center frequency set to be the resonant frequency of odd mode, which can be expressed as $f_{\text{odd}} = f_0(1 - M_{11} \times \Delta f/2f_0)$. At this step, one can specify the values of ϑ_C, Z_1, and ϑ_1 and obtain the values of Z_{oe} and Z_{oo} by an analytical method [8]. Second, put the open stub back. The two parameters of the open stub, i.e., Z_2 and ϑ_2, can be adjusted to achieve the desired resonant frequency and the needed external coupling strength of the

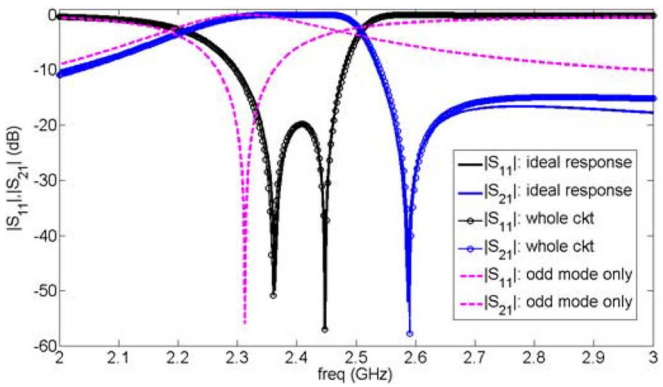

Fig. 3. Responses generated from the coupling matrix and from electrical network shown in Fig. 2(a) with synthesis parameters.

even mode. Here, the resonant frequency of the even mode is $f_{\text{even}} = f_0(1 - M_{22} \times \Delta f/2f_0)$.

To illustrate the procedure, an example is taken of a second-order generalized Chebyshev filter with a passband return loss of 20 dB and a single transmission zero at a normalized frequency $\Omega = 3$. The corresponding coupling coefficients are $M_{S1} = 1.1110$, $M_{S2} = 0.6170$, $M_{11} = 1.4545$, and $M_{22} = -1.6260$. For filter with center frequency $f_0 = 2.4$ GHz and fractional bandwidth $\text{FBW} = 0.05$, the ideal response is depicted in Fig. 3 as solid lines. After getting the coupling matrix, ϑ_C could first be specified. Here, we set $\vartheta_C = 60°$, $Z_1 = 50\ \Omega$, and $\vartheta_1 = 60°$ and obtain $Z_{oe} = 75.2552\ \Omega$ and $Z_{oo} = 38.1022\ \Omega$ for a uniform impedance resonator with characteristic impedance $Z_c = 50\,\Omega$ at frequency $f_{\text{odd}} = 2.3127$ GHz. Next, put the open stub back and adjust the values of Z_2 and ϑ_2 by the optimization method to let the response of the circuit match with the ideal response calculated from the M matrix. The optimized values of Z_2 and ϑ_2 are $62\,\Omega$ and $86.8°$, respectively, at frequency $f_{\text{even}} = 2.4976$ GHz. According to the obtained electrical parameters in Fig. 2(a), the corresponding response is shown in Fig. 3 as circled lines. The frequency response contributed only by the odd mode is also depicted in Fig. 3 as dashed lines to let us understand the procedures clearer.

B. Extended-Doublet Filters

Based on the doublet filters developed in Section II-A, the emphasis here is put on how to extend the design to extended-doublet filters [4]. There are two possible arrangements suitable to form extended-doublet filters. One possible arrangement is indicated in Fig. 4, where the extended doublet filter consists of a doublet filter plus a grown resonator. The grown resonator is a half-wavelength resonator with both ends open. In this case, the grown resonator would mainly couple to the odd mode of the E-shaped resonator. For the even mode of the E-shaped resonator, it acts as a nonresonant element, which slightly perturbs the resonant frequency of the even mode. Another possible design is shown in Fig. 5 where both ends of the grown resonator are shorted to ground. In this case, the grown resonator mainly couples to the even mode of the E-shaped resonator and acts as a nonresonant element to the odd mode of the E-shaped resonator.

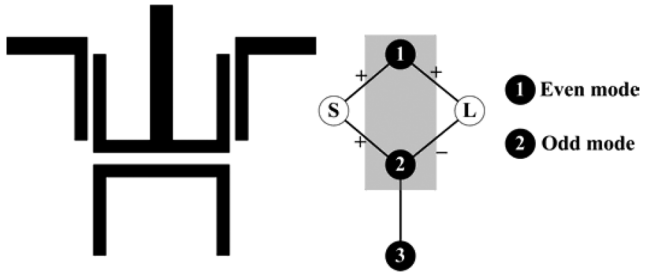

Fig. 4. Layout of extended-doublet filter and its corresponding coupling scheme. The design is for flat group-delay response.

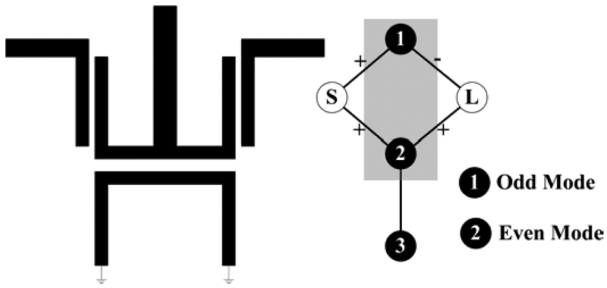

Fig. 5. Layout of extended-doublet filter and corresponding coupling scheme. The design is for skirt selectivity response.

To clarify the coupling relationship between each resonator, the coupling routes are accompanied with layouts in Figs. 4 and 5.

The extended-doublet filter has a pair of finite transmission zeros [4]. For the design in Fig. 4, the pair of transmission zeros is on the imaginary-frequency axis. On the other hand, to generate a pair of real-frequency transmission zeros, the design in Fig. 5 must be adopted. The difference between the two designs can be understood from the governing equation of finite transmission zeros. Since the proposed extended doublet filters are symmetric structures, the relations $|M_{S1}| = |M_{1L}|$ and $|M_{S2}| = |M_{2L}|$ always hold. Thus, the governing equation of finite transmission zero can be expressed as

$$\Omega^2 = \frac{M_{S1}^2 M_{23}^2}{M_{S1}^2 - M_{S2}^2}. \tag{5}$$

As discussed in the design of the doublet, the coupling coefficient of source to odd mode is stronger than that of source to even mode. Thus, for the design in Fig. 4, $|M_{S2}| > |M_{S1}|$, which leads to $\Omega^2 < 0$. On the contrary, for the design in Fig. 5, $|M_{S2}| < |M_{S1}|$, which results in $\Omega^2 > 0$. In conclusion, the design in Fig. 4 can be used to generate delay-flattening transmission zeros, while the design in Fig. 5 can be used to generate a pair of attenuation poles.

To illustrate the procedure of design, a generalized Chebyshev filter with passband return loss of 20 dB and a pair of transmission zeros at $\Omega = \pm 2$ is taken as an example. The design of an extended doublet starts from the synthesis of the coupling matrix, which can be done using the technique in [9]. The synthesized coupling matrix is shown in Fig. 6(a). Using the information of M_{S1} and M_{S2}, one can construct the doublet by the method provided in Section II-A. Excluding M_{23} and M_{32} in the coupling matrix, one can calculate the response contributed

M	S	1	2	3	L
S	0	0.8613	0.6202	0	0
1	0.8613	0	0	0	-0.8613
2	0.6202	0	0	1.3878	0.6202
3	0	0	1.3878	0	0
L	0	-0.8613	0.6202	0	0

(a)

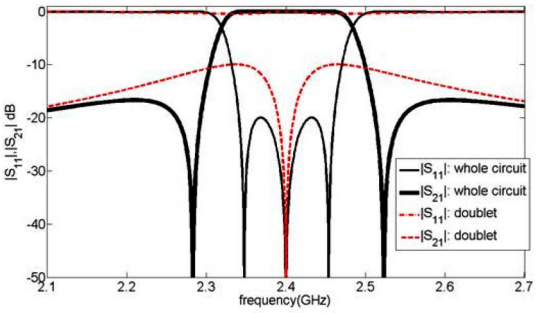

(b)

Fig. 6. Extended-doublet filter with in-band return loss RL = 20 dB, normalized transmission zeros at $\Omega = \pm 2$. (a) Its coupling matrix. (b) Responses of extended doublet filter and responses contributed by doublet only.

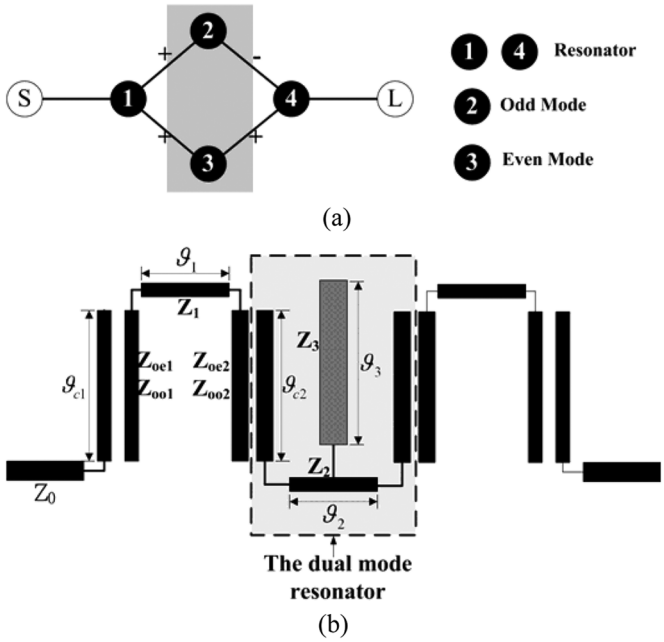

(a)

(b)

Fig. 7. Box-section filter. (a) Filter's coupling scheme. (b) Proposed layout.

from the doublet only. For instance, if the center frequency and fractional bandwidth of the designed filter are 2.4 GHz and 5%, respectively, the responses of the doublet are shown as dotted lines in Fig. 6(b). After getting the initial design of the doublet, add the grown resonator. Since $\Omega^2 > 0$ in this case, the layout in Fig. 5 must be adopted. Ideally, the response of the extended doublet would be the solid lines shown in Fig. 6. The physical implementation of this design will be presented in Section III to confirm the validity.

C. Box-Section Filters

The fourth-order filter in the "box-section" configuration was first proposed in [2] and realized by coaxial resonators. With the zero-shifting property, it is possible to use the similar filter structure to realize the finite transmission zero either on the upper or lower stopband. The box-section filter is suitable for the complementary filters of a transmit/receive duplexer [7] since it has an asymmetric response with high selectivity on one side of the passband. The microstrip box-section filter was first reported in [6] with open square loop resonators. Since the box-section coupling diagram is symmetric where $M_{S1} = M_{4L}, M_{12} = -M_{24}$, $M_{13} = M_{34}$, and $M_{11} = M_{44}$ should be held in the coupling route shown in Fig. 7(a). Therefore, it is preferable to layout the filter symmetrically because a symmetrical-layout filter can inherently obtain symmetrical coupling coefficients. The asymmetrical layout causes the filters in [6] to be difficult to keep the coupling coefficients symmetric. Another microstrip box-section filter was proposed in [7]. Although the layout of the filters in [7] is symmetric, it suffers from a spurious response in the filter's lower stopband due to one of the filter's resonators being a higher order mode resonator. In this paper, the layout depicted in Fig. 7(b) solves the problems mentioned. The E-shaped resonator is symmetric and is free from lower stopband spurious resonances. Due to the symmetry, only half of the electrical parameters are shown in Fig. 7(b). As explained in the doublet filter, the circuit layout in Fig. 7(b) satisfies the required sign of couplings.

To illustrate how to obtain the corresponding electrical parameters in Fig. 7(b) from a prescribed response, examples are taken as follows. The first example is a fourth-order generalized Chebyshev filter with a passband return loss of 20 dB, and a single transmission zero at $\Omega = -2.57$, which gives a lobe level of -48 dB on the lower side of the passband. The corresponding coupling matrix M is shown in Fig. 8(a). After the low-pass-to-bandpass transformation, the ideal bandpass response of this filter with a center frequency of 2.4 GHz and fractional bandwidth of 5% is shown in Fig. 8(b).

The design procedures are described as follows. First, remove the open stub in the E-shaped resonator in Fig. 7(b), which is equivalent to discarding the even mode [resonator 3 in Fig. 7(a)] of the E-shaped resonator. After removing the open stub, the circuit becomes a third-order hairpin-like filter. The coupling matrix M_1 of this hairpin-like filter is identical to the coupling matrix M in Fig. 8(a), except M_{3i} and M_{i3} are zero. The ideal response of this hairpin-like filter can be calculated from the M_1 matrix, as denoted by circled lines in Fig. 8(b). To get the electrical parameters associated with the asynchronously tuned third-order hairpin-like filter, a synchronous tuned third-order hairpin filter provides the initial design and is synthesized first. The synchronous tuned hairpin filter has the coupling matrix M_2, which is identical to M_1, except $M_{ii} = 0$. When synthesizing the synchronously tuned hairpin filter, we set $\vartheta_{C1} = 90°$, $\vartheta_{C2} = 60°$, $Z_1 = 50\ \Omega$, and $Z_2 = 50\ \Omega$ at $f = f_0$, and the characteristic impedance of each resonator to 50 Ω. With these settings, the electrical parameters of the synchronously tuned hairpin filter are calculated and shown in Table I(a), which provides the initial values for the asynchronous-tuned hairpin-like filter. An optimization routine is then involved. The goal of the

M	S	1	2	3	4	L
S	0	1.0343	0	0	0	0
1	1.0343	-0.0342	0.7291	0.5441	0	0
2	0	0.7291	-0.5572	0	-0.7291	0
3	0	0.5441	0	0.8282	0.5441	0
4	0	0	-0.7291	0.5441	-0.0342	1.0343
L	0	0	0	0	1.0343	0

(a)

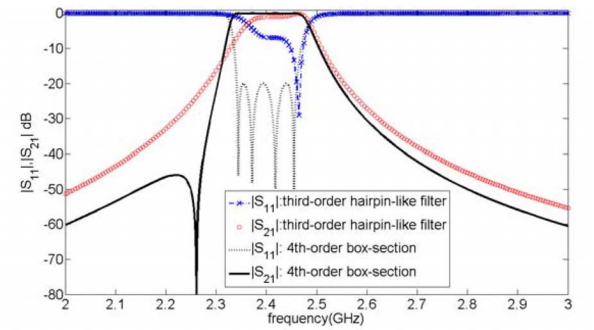

(b)

Fig. 8. Fourth-order box-section filter. (a) Its coupling matrix. (b) Responses of the box-section filter and ideal responses of the asynchronous tuned third-order hairpin-like filter calculated by M_1 matrix.

TABLE I

ELECTRICAL PARAMETERS CORRESPONDING TO BOX-SECTION FILTERS SHOWN IN FIG. 7(b). HERE, $\vartheta_{C1} = 90^o$, $\vartheta_{C2} = 60^o$, $Z_1 = 50\ \Omega$, AND $Z_2 = 50\ \Omega$. ALL OF THE ELECTRICAL LENGTHS CORRESPOND TO THE CENTER FREQUENCY OF THE FILTER. DESIGN 1: IN-BAND RETURN LOSS $\mathrm{RL} = 20$ dB, $\Omega = -2.57$, AND $\mathrm{FBW} = 5\%$ DESIGN 2: IN-BAND RETURN LOSS $\mathrm{RL} = 20$ dB, $\Omega = 2.57$, AND $\mathrm{FBW} = 5\%$

	Initial values	Design #1	Design #2
Z_{oe1} (ohm)	68.6941	68.6967	68.6169
Z_{oo1} (ohm)	39.7079	39.7204	39.7758
Z_{oe2} (ohm)	53.5286	54.2217	52.5632
Z_{oo2} (ohm)	46.9091	47.5517	46.0413
ϑ_1 (degrees)	30	30.2141	29.7113
ϑ_2 (degrees)	60	58.1787	61.635
Z_3 (ohm)	NaN	19.1823	20.2808
ϑ_3 (degrees)	NaN	95.9949	84.3721

optimization routine is to find a set of electrical parameters, which can make the response match with the response of the ideal asynchronously tuned hairpin-like filter calculated from the M_1 matrix. The optimized parameters are shown in Table I for comparison. Note that the optimized values of associated parameters are nearly identical to the initial values; therefore, the optimization routine can converge within a few times. Finally, put the open stub back and optimize the parameters Z_3 and ϑ_3 to make the response match with the response of the desired box-section filter's response, as denoted by solid lines in Fig. 8(b). The optimized values of Z_3 and $_3$ are given in Table I as well.

Instead of a low-pass prototype filter with a transmission zero at $\Omega = -2.57$ in the first example, the second example locates the transmission zero at a normalized frequency $\Omega = 2.57$

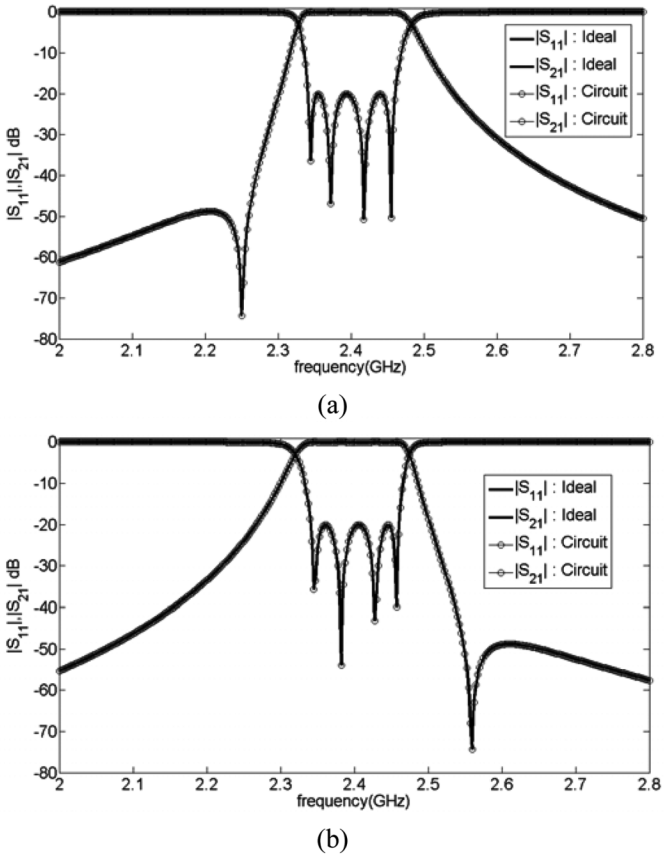

(a)

(b)

Fig. 9. Responses of the box-section filters. (a) Responses obtained by electrical parameters of design #1 in Table I and its coupling matrix, respectively. (b) Responses obtained by electrical parameters of design #2 in Table I and its coupling matrix, respectively.

and keeps all other parameters unchanged. According to the synthesis procedures in [2], the inter-resonator couplings are unchanged, but self-couplings [principal diagonal matrix elements, $M_{11}, M_{22}, \ldots$, etc., of the coupling matrix in Fig. 8(a)] must change sign. Following the same procedures in the previous design, one can get the electrical parameters given in Table I. In Table I, the column of design #1 corresponds to a low-pass prototype filter transmission zero at $\Omega = -2.57$ and the column of design #2 corresponds to a low-pass prototype filter transmission zero at $\Omega = -2.57$. The responses obtained from the electrical parameters are listed in Table I and responses calculated from the M matrix in Fig. 8(a) are both plotted in Fig. 9 for comparison.

III. DESIGN EXAMPLES AND EXPERIMENTAL RESULTS

The extended-doublet filter discussed in Section II-B with its ideal response. shown in Fig. 6, and the design #1 of box-section filter discussed in Section II-C with its ideal response, shown in Fig. 9(a), are fabricated to verify the designs. Although all of the electrical parameters obtained in Section II can be transformed to physical parameters, it does not include the junction effect. Therefore, a commercial electromagnetic (EM) simulator Sonnet [11] is adopted to take all the EM effects into consideration. To efficiently tune the physical dimensions of the filter to achieve the prescribed response, the diagnosis and tuning

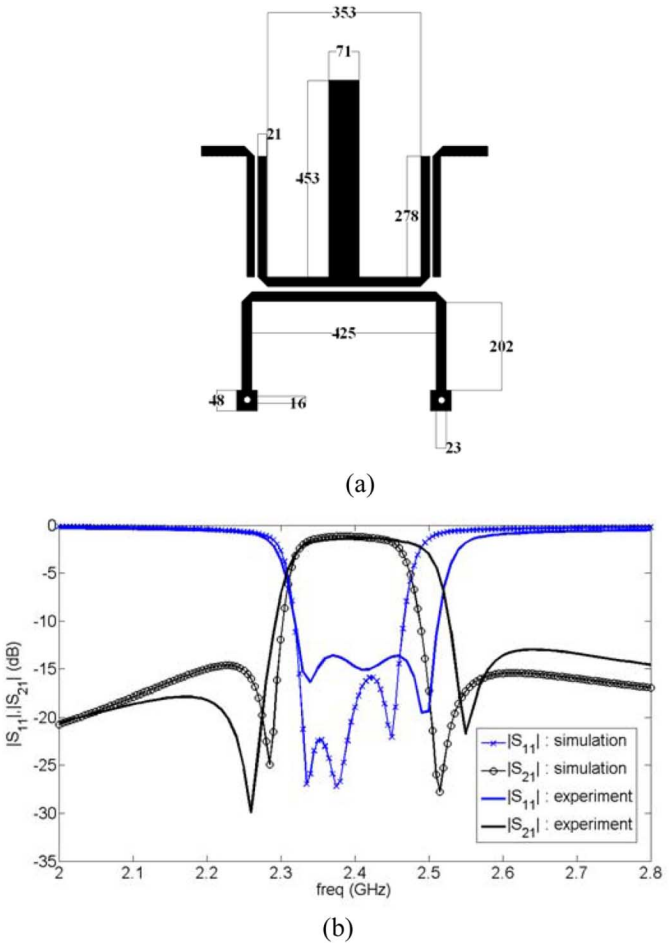

Fig. 10. Fabricated extended-doublet filter. (a) Layout (unit: mils). (b) Simulated and measured response.

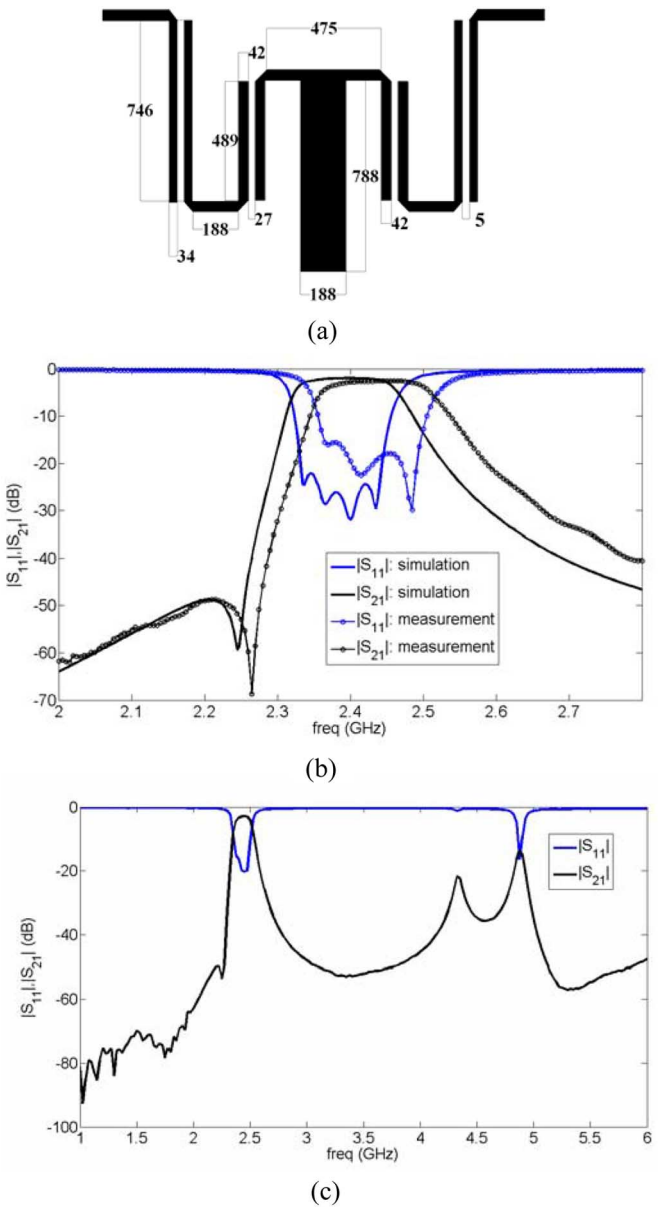

Fig. 11. Fabricated box-section filter. (a) Layout (unit: mil). (b) Simulated and measured response. (c) Measured wideband response.

Fig. 12. Possible filter layout that can be modeled as a doublet configuration.

methods proposed in [12] are taken. Fig. 10 shows the physical dimensions and the corresponding responses for the extended-doublet filter where an RO6010 substrate with a dielectric constant of 10.8 and thickness of 50 mil is used. Fig. 11 depicts the physical dimensions and corresponding responses for the box-section filter where an RO4003 substrate with a dielectric constant of 3.63 and a thickness of 20 mil is used. The measured in-band insertion loss of the filters in Figs. 10 and 11 are 1.4 and 2.7 dB, respectively. In Fig. 10(b), the experimental results show a larger passband than the simulated ones. The deviation mainly results from the fabrication error. In Fig. 11(b), the measured response is shifted about 30 MHz. Further investigation showed that the dielectric constant of the substrate is closer to 3.4 rather than 3.63. The wideband measurement results of the fabricated box-section filter are shown in Fig. 11(c).

IV. Discussion

In Section II, we have discussed how to get the electrical parameters of a filter network in a doublet, an extended-doublet, and a box-section configuration from the corresponding coupling matrices. With the understanding of the correspondence between the coupling matrix and physical structure, the layout is not limited to those provided in this paper. A filter can be modeled by the box-like coupling scheme, as long as it contains a two-mode resonator that is physically symmetric and supports two resonant modes. For instance, the filters in Fig. 12 can also be modeled as a doublet filter since it is symmetric and has two resonant modes. However, for the filter in Fig. 12, it is not easy to get the initial physical dimensions. On the contrary, the initial dimensions of the layouts proposed in this paper can easily

be obtained. Besides, using the E-shaped resonator and the design procedures provided in this paper, all electrical parameters of a filter with box-like coupling schemes can be easily obtained. These parameters can be applied to filters with the same low-pass prototype and fractional bandwidth, but a different center frequency and a different substrate. Having clear initial dimensions of a filter can save quite a lot of time in the design when comparing to the conventional design procedures of cross-coupled filters, e.g., the filters in [5]. In the design of a conventional cross-coupled filter, once the substrate, shape of the resonator, or center frequency of a filter is changed, one must redo the design from the very beginning of the procedures.

The sensitivity analysis of the box-like coupling routes can be performed by the method proposed in [13]. The most sensitive part of the proposed structures is the coupling section between the E-shaped resonator and the source/load or other resonators because the coupling section controls the coupling strengths of two modes of the E-shaped resonator to an external circuit simultaneously.

V. Conclusion

The three box-like coupling schemes, namely, the doublet, extended doublet, and box section, have been illustrated. How an E-shaped resonator constructs the box-like portion of the coupling schemes has been explained. The couplings between an E-shaped resonator, external feeding network, and other single-mode resonators have also been modeled. The correspondence between an electrical network and coupling matrix has been established, which make it possible to get the initial dimensions of a filter from the information of a coupling matrix. Besides, with the aid of a proper coupling matrix served as a surrogate model, a systematic way of tuning a filter has been applied, which saves a lot of time for optimizing the response of a filter. The proposed filters have provided an effective way to design a class of filters exhibiting a generalized Chebyshev response to meet the stringent specification in modern communication systems.

References

[1] J. S. Hong and M. J. Lancaster, *Microstrip Filters for RF/Microwave Applications*. New York: Wiley, 2001.

[2] R. J. Cameron, A. R. Harish, and C. J. Radcliffe, "Synthesis of advanced microwave filters without diagonal cross-couplings," *IEEE Trans. Microw. Theory Tech.*, vol. 50, no. 12, pp. 2862–2872, Dec. 2002.

[3] U. Rosenberg and S. Amari, "Novel coupling schemes for microwave resonator filters," *IEEE Trans. Microw. Theory Tech.*, vol. 50, no. 12, pp. 2896–2902, Dec. 2002.

[4] S. Amari and U. Rosenberg, "New building blocks for modular design of elliptic and self-equalized filters," *IEEE Trans. Microw. Theory Tech.*, vol. 52, no. 2, pp. 721–736, Feb. 2004.

[5] J. S. Hong and M. J. Lancaster, "Couplings of microstrip square open-loop resonators for cross-coupled planar microwave filters," *IEEE Trans. Microw. Theory Tech.*, vol. 44, no. 12, pp. 2099–2108, Dec. 1996.

[6] S. Amari, G. Tadeson, J. Cihlar, R. Wu, and U. Rosenberg, "Pseudo-elliptic microstrip line filters with zero-shifting properties," *IEEE Microw. Wireless Compon. Lett.*, vol. 14, no. 7, pp. 346–348, Jul. 2004.

[7] A. G. Lamperez and M. S. Palma, "High selectivity X-band planar diplexer with symmetrical box section filters," in *Eur. Microw. Conf.*, Paris, France, Oct. 2005, vol. 1, pp. 105–108.

[8] J. R. Lee, J. H. Cho, and S. W. Yun, "New compact bandpass filter using microstrip $\lambda/4$ resonator with open stub inverter," *IEEE Microw. Guided Wave Lett.*, vol. 12, no. 12, pp. 526–527, Dec. 2000.

[9] R. J. Cameron, "Advanced coupling matrix synthesis techniques for microwave filters," *IEEE Trans. Microw. Theory Tech.*, vol. 51, no. 1, pp. 1–10, Jan. 2003.

[10] M. Makimoto and S. Yamashita, *Microwave Resonators and Filters for Wireless Communication*. New York: Springer, 2001.

[11] *Em User's Manual*. Liverpool, NY: Sonnet Software Inc., 2004.

[12] A. G. Lamperez, S. L. Romano, M. S. Palma, and T. K. Sarka, "Fast direct electromagnetic optimization of a microwave filter without diagonal cross-couplings through model extraction," in *Eur. Microw. Conf.*, Munich, Germany, 2003, vol. 2, pp. 1361–1364.

[13] S. Amari and U. Rosenberg, "On the sensitivity of coupled resonator filters without some direct couplings," *IEEE Trans. Microw. Theory Tech.*, vol. 51, no. 6, pp. 1767–1773, Jun. 2003.

Ching-Ku Liao was born in Taiwan, R.O.C., on October 16, 1978. He received the B.S. degree in electrophysics and M.S. degree in communication engineering from National Chiao-Tung University, Hsinchu, Taiwan, R.O.C., in 2001 and 2003, respectively, and is currently working toward the Ph.D. degree in communication engineering at National Chiao-Tung University.

Since March 2006, he has been a Visiting Researcher with University of Florida, Gainesville, under a sponsorship of the National Science Council Graduate Student Study Abroad Program (GSSAP). His research interests include the analysis and design of microwave and millimeter-wave circuits.

Pei-Ling Chi was born in Taiwan, R.O.C., on March 25, 1982. She received the B.S. and M.S. degrees in communication engineering from National Chiao Tung University, Hsinchu, Taiwan, R.O.C., in 2004 and 2006, respectively, and is currently working toward the Ph.D. degree in electrical engineering at the University of California at Los Angeles.

Her research interests include the analysis and design of microwave and millimeter-wave circuits.

Chi-Yang Chang (S'88–M'95) was born in Taipei, Taiwan, R.O.C., on December 20, 1954. He received the B.S. degree in physics and M.S. degree in electrical engineering from National Taiwan University, Taipei, Taiwan, R.O.C., in 1977 and 1982, respectively, and the Ph.D. degree in electrical engineering from the University of Texas at Austin, in 1990.

From 1979 to 1980, he was with the Department of Physics, National Taiwan University, as a Teaching Assistant. From 1982 to 1988, he was with the Chung-Shan Institute of Science and Technology (CSIST), as an Assistant Researcher, where he was in charge of development of microwave integrated circuits (MICs), microwave subsystems, and millimeter-wave waveguide E-plane circuits. From 1990 to 1995, he returned to CSIST as an Associate Researcher in charge of development of uniplanar circuits, ultra-broadband circuits, and millimeter-wave planar circuits. In 1995, he joined the faculty of the Department of Communication, National Chiao Tung University, Hsinchu, Taiwan, R.O.C., as an Associate Professor and became a Professor in 2002. His research interests include microwave and millimeter-wave passive and active circuit design, planar miniaturized filter design, and monolithic microwave integrated circuit (MMIC) design.